54 KSME Journal, Vol.4, No.1, pp. 54~61, 1990.

NUMERICAL SIMULATION OF THE HYDRODYNAMICALLY DEVELOPING FLOW OF A VISCOELASTIC FLUID

Y. Na* and J.Y. Yoo*

(Received October 14, 1989)

Hydrodynamically developing flow of Oldroyd *B* fluid in the planar die entrance region has been investigated numerically using SIMPLER algorithm in a non-uniform staggered grid system. It has been shown that for constant values of the Reynolds number, the entrance length increases as the Weissenberg number increases. For small Reynolds number flows the center-line velocity distributions exhibit overshoot near the inlet, which seems to be related to the occurrence of numerical breakdown at small values of the limiting Weissenberg number than those for large Reynolds number flows. The distributions of the first normal stress difference display the development of the flow characteristics from extensional flow to shear flow.

Key Words: Hydrodynamically Developing Flow, Viscoelastic Fluid, Oldroyd *B* Fluid, SIMPLER Algorithm, Modified Hybrid Scheme

NOMENCLATURE

$\underline{D}$	: Rate of strain tensor
$\underline{L}$	: Slit halfheight
P	: Pressure, indeterminate part of the Cauchy stress tensor
R	: The Reynolds number
t	: Time
U	: Average velocity in the slit
$\underline{u}$	: Velocity vector
u,v	: Velocity components
W	: The Wissenberg number based on the difference between stress relaxation time and retardation time
W_1	: The Weissenberg number based on stress relaxation time
x,y	: Tectangular Cartesian coordinates
ϵ	: Tatio of retardation time to stress relaxation time
η	: Zero-shear-rate viscosity, $\eta_1+\eta_2$
η_1	: Non-Newtonian contribution to η
η_2	: Newtonian contribution to η
λ_1	: Stress relaxation time
λ_2	: Ratardation time
ρ	: Density
(σ, γ, τ)	: xx, yy and xy components of $\underline{\tau}_1$, respectively
$\underline{\tau}$	: Determinate part of the Cauchy stress tensor
$\underline{\tau}_1$	: Non-Newonian contribution to $\underline{\tau}$
$\underline{\tau}_2$	: Newtonian contribution to $\underline{\tau}$

1. INTRODUCTION

In manufacturing processes of thermoplastic products by way of extrusion or injection molding, distortion of polymer is an important phenomenon. The type and severity of distortion depends on the properties of polymer melts and the processing conditions. Attempts to simulate the processing conditions through the die can be made by considering the hydrodynamically developing flows of viscoelastic fluids in planar and axisymmetric entrance regions. Comprehensive discussions on this problem, well treated for inelastic fluids, have not been comparably treated for viscoelastic fluids. Numerical simulations of the hydrodynamically developing flow of viscoelastic fluids between parallel plates have been reported in only a few studies. Chang et al. (1979) used the Galerkin FEM for the creeping flow of White-Metzner fluid, but could obtain only Newtonian solution due to numerical instability. Mendelson used the same method for the creeping flow of convected Maxwell fluid and obtained the solution for very low values of elasticity parameter (Mendelson et al., 1982). Gaidos and Darby (1988) used finite element collocation method for the non-creeping flow of a modified White-Metzner fluid, where the model parameters were obtained from accurate experimental data.

Most experimental studies involving viscoelastic fluids consist of observations and measurements of the phenomena occurring due to the change of the flow rate of the same fluid. Therefore, in some situations the inertia may become an important factor. But most previous numerical studies on viscoelastic flows, especially those using finite element method have traditionally neglected the inertia terms. Recently, Joseph et al. (1985) and Yoo et al. (1985)suggested that the differential equations governing the flow of Oldroyd fluid models with instantaneous elasticity may change their type when the inertia terms are included. Based on this finding, Song and Yoo(1987) and Choi et al. (1988) showed that type dependent difference methods can be successfully applied for the numerical simulation of the planar contraction flows of upper convected Maxwell fluid and one-mode Giesekus fluid, respectively, both of them having instantaneous elasitcity, i.e., without retardation time. The purpose of the present study is to simulate the hydrodynamically devel-

*Department of Mechanical Engineering, Seoul National University, Seoul, 151~742, Korea

oping flow of an incompressible viscoelastic fluid with retardation time between parallel plates, using finite difference method and taking into account of the inertia terms. To consider separately the elasticity effect of the viscoelastic fluid without shear thinning effect, Oldroyd B fluid model is used.

2. PROLBLEM STATEMENT

2.1 Governing Equations

The constitutive model used is Oldroyd B fluid model which can be expressed as follows:

$$\underline{\tau}+\lambda_1\overset{\nabla}{\underline{\tau}}=2\eta(\underline{D}+\lambda_2\overset{\nabla}{\underline{D}}) \tag{1}$$

where $\overset{\nabla}{\underline{\tau}}=\frac{\partial\underline{\tau}}{\partial t}+\underline{u}\cdot\nabla\underline{\tau}-\underline{\tau}\cdot\nabla\underline{u}-\nabla\underline{u}^T\cdot\underline{\tau}$
and $\underline{D}=1/2(\nabla\underline{u}+\nabla\underline{u}^T)$.

If $\lambda_2=0$, the model reduces to a convected Maxwell model and if $\lambda_1=\lambda_2$, to a Newtonian fluid with viscosity η. The stress tensor $\underline{\tau}$ can be conveniently decomposed into two parts as follows:

$$\underline{\tau}=\underline{\tau}_1+\underline{\tau}_2 \tag{2}$$

where $\underline{\tau}_1$ and $\underline{\tau}_2$ are non-Newtonian and Newtonian contributions to $\underline{\tau}$, respectively, such that

$$\underline{\tau}_1+\lambda_1\overset{\nabla}{\underline{\tau}}_1=2\eta_1\underline{D}, \tag{3}$$
$$\underline{\tau}_2=2\eta_2\underline{D}, \tag{4}$$

and it can be readily shown that $\eta=\eta_1+\eta_2$ and $\lambda_2=\eta_2\lambda_1/(\eta_1+\eta_2)$.

By substituting equation (2) into (1), the continuity, momentum and constitutive equations of Oldroyd B model are now written as

$$\nabla\cdot\underline{u}=0, \tag{5}$$
$$\rho(\frac{\partial\underline{u}}{\partial t}+\underline{u}\cdot\nabla\underline{u})=-\nabla P+\nabla\cdot\tau_1+\eta_2\nabla^2\underline{u}_2, \tag{6}$$
$$\underline{\tau}_1+\lambda_1(\frac{\partial\underline{\tau}_1}{\partial t}+\underline{u}\cdot\nabla\underline{\tau}_1-\nabla\underline{u}^T\cdot\underline{\tau}_1-\underline{\tau}_1\cdot\nabla\underline{u})$$
$$=\eta_1(\nabla\underline{u}+\nabla\underline{u}^T). \tag{7}$$

2.2 Nondimensionalization

The physical variables can be nondimensionalized by introducting L, U and $\eta U/L$ as scales for length, velocity and stress and by defining the Reynolds number and the Weissenberg number as follows:

$$R=\frac{\rho UL}{\eta},\quad W=\frac{\lambda_1 U}{L}(1-\frac{\lambda_2}{\lambda_1}).$$

We further introduce.

$$W_1=\frac{\lambda_1 U}{L},\quad \epsilon=\frac{\lambda_2}{\lambda_1}.$$

Thus, the system of Eqs. (5, 6, 7) is now written in dimensionless form as

$$u_x+v_y=0 \tag{8}$$
$$(Ruu-\epsilon u_x)_x+(Rvu-\epsilon u_y)_y=-P_x+\sigma_x+\tau_y, \tag{9}$$
$$(Ruv-\epsilon v_x)_x+(Rvv-\epsilon v_y)_y=-P_y+\tau_x+\gamma_y, \tag{10}$$
$$(1-2W_1u_x)\sigma+W_1(u\sigma_x+v\sigma_y)$$
$$=2(1-\epsilon)u_x+2W_1u_y\tau, \tag{11}$$
$$\tau+W_1(u\tau_x+v\tau_y)=W_1v_x\sigma+W_1u_y\gamma$$
$$+(1-\epsilon)v_x+(1-\epsilon)u_y, \tag{12}$$
$$(1-2W_1v_y)\gamma+W_1(u\gamma_x+v\gamma_y)$$
$$=2(1-\epsilon)v_y+2W_1v_x\tau, \tag{13}$$

where subscripts denote differentiation.

2.3 Boundary Conditions

We now describe the boundary conditions on each of the four boundaries shown in Fig.1. We note that the unbounded problem domain $0<x<\infty$ and $0<y<1$ is represented by a finite domain $0<x<10$ and $0<y<1$, based on the assumption that the flows will become fully developed within $x<10$, which will be found to be valid later.

(1) Inlet ($x=0$, $0<y<1$)

In the classical entry length problem, the flow in the inlet section is assumed to be plug flow. Thus, the velocity component u is discontinuous at the entrance corner and the pressure is infinite there. This singularity can be removed by specifying a continuous entrance velocity profiile which approximates plug flow, while also preserves the no slip boundary condition at the wall (Gaidos and Darby, 1988). The inlet velocity profile can then be approximated as a piecewise continuous polynomial:

$$u(y)=\begin{cases}c_1 & \text{for } 0<y<y_c,\\ c_2+c_3y+c_4y^2 & \text{for } y_c<y<1,\end{cases}$$

where the coefficients are determined by satisfying the no slip condition at $y=1$, by requiring the continuity of both the velocity and velocity gradient at $y=y_c$, and by considering the mass balance $\int u(y)dy=1$. The resulting inlet velocity profile for $y_c=0.8714$ is

$$u(y)=\begin{cases}1.0448 & \text{for } 0<y<y_c,\\ -46.92+110.09y-63.17y^2 & \text{for } y_c<y<1,\end{cases} \tag{14}$$

The values of σ, τ and γ are obtained from Eqs.(11, 12, 13) by considering $v=u_x=0$ at the inlet and by assuming that $\sigma_x=\tau_x=\gamma_x=0$ in the immediate upstream region of the inlet;

$$\gamma=0,\ \tau=(1-\epsilon)u_y,\ \sigma=2W_1(1-\epsilon)u_y^2. \tag{15}$$

(2) Solid wall parallel to the x-axis ($0<x<10$, $y=1$).

The values of σ, τ and γ are obtained in terms of u_y from Eqs.(11, 12, 13) under the no-slip conditions $u=v_x=v_y=u_x=0$:

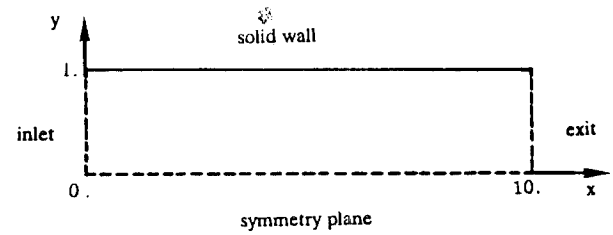

Fig. 1 Boundaries of the flow field

$$\gamma=0,\ \tau=(1-\epsilon)\,u_y,\ \ \sigma=2W_1(1-\epsilon)\ u_y^2 \tag{16}$$

(3) Plane of symmetry ($0<x<10,\ y=0$).

On the plane of symmetry we have $u_y=v=v_x=\tau=0$. The stress components σ and γ are obtained by solving the following nonlinear ordinary differential equations which are derived from Eqs.(11) and (13) under the symmetry conditions aforementioned:

$$\begin{aligned}&(1-2W_1u_x)\sigma+W_1u\sigma_x=2(1-\epsilon)\,u_x,\\&(1-2W_1v_x)\sigma+W_1u\gamma_x=2(1-\epsilon)\,v_x.\end{aligned} \tag{17}$$

(4) Exit ($x=10,\ 0<y<1$)

At the exit, Neumann conditions $\mu_x=u_x=\tau_x=\gamma_x=0$ are imposed.

3. NUMERICAL METHOD

We recall that in Eqs.(9, 10) the Newtonian part of the stress is treated as diffusion terms so that these and the convective terms together appear in conservative forms. Thus, it is appropriate for us to apply a finite volume method involving SIMPLER algorithm(Patankar, 1980)on a staggered non-uniform grid system.

3.1 Momentum Equations

In discretizing the convection-diffusion terms of the momentum equation, a slightly modified version of the hybrid scheme has been empoyed by Na(1989). In the conventional hybrid scheme, the coefficients of the difference equations are kept to be always positive and the diffusion terms are totally neglected when the cell Peclet number exceeds certain reference value. But, since we are now considering the viscoelastic fluids with retardation time, the omission of η_2 may lead us to entirely different fluids, such as upper convected Maxwell fluids. Therefore, in order to keep the diffusion terms all the time, we discretize them by CD(central difference) and the convection terms by either CD or UD(upwind difference). In orther words, when the cell Peclet number is larger than some reference value, UD is taken for the convection terms and when it is smaller, CD is taken for them as shown below:

$$\underbrace{(Ruu-\epsilon u_x)_x+(Rvu-\epsilon u_y)_y}_{\text{modified HS(CD or UD)}}=\underbrace{-P_x+\sigma_x+\tau_y}_{\text{source term(CD)}}$$

3.2 Pressure and Pressure Correction Equations

In calculating the velocity components through SIMPLER algorithm, both the pressure and pressure correction equations need to be formulated. The detailed procedure for deriving these equations for Newtonian fluids by making use of the continuity Eq. (8) is explained in Patankar (1980). This algorithm has been modified by Na(1989) to incorporate the non-Newtonian controbution to the stress in the source terms of the pressure and pressure correction equations.

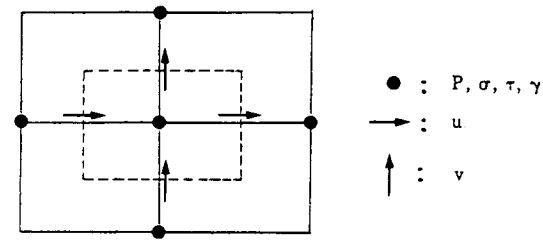

Fig. 2 Staggered grid

3.3 Constitutive Equations

The constitutive Eqs.(11, 12, 13)for the non-Newtonian part of the stress have been discretized by the same method as used in Choi et al.(1988) , which introduces an upwind corrected scheme involving an artificial viscosity term to attain second-order accuracy and unconditional stability. On the plane of symmetry the boundary conditions for σ and γ have to be given by solving the two nonlinear ordinary differential Eq. (17). Those equations are solved by the backward Euler method which ensures the stability of the solution (Choi et al, 1988)

3.4 Grid System

In SIMPLER algorithm, the pressure and stress components are represented in terms of velocity components, and vice versa. Therefore a staggered grid, as shown in Fig. 2, is used, where the nodes for the pressure and stress components (hereafter called as scalar nodes) are marked with closed circles, while the nodes for u and v are marked with horizontal and vertical arrows, respectively.

In the entry length problem, velocity gradient is steeper near the wall than in the central region. Thus, a non-uniform grid system with finer meshes near the wall is preferred to a uniform grid system. In Fig. 3, a non-uniform 40×20 grid system for scalar nodes used in the present study is shown.

3.5 Solution of the nonlinearly Coupled System

The resulting nonlinearly coupled system is solved by employing a line-by-line iteration techniqe. In the inner iteration of the linearized equations for u, v, P, σ, τ and γ, under-relaxation parameters are used and appropriate artificial viscosity terms are included. In each step of inner iteration of momentum equations and constitutive equations, values of boundary stress are needed and calculated in terms of velocity field.

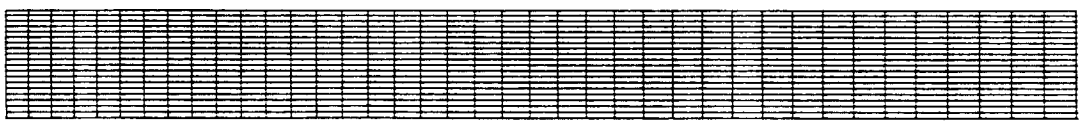

Fig. 3 Non-uniform grid system for scalar nodes used in the present study

4. RESULTS AN DISCUSSIONS

Although the entry length problem has been extensively investigated for inelastic fluids, it has not been comparably studied for viscoelastic fluids, despite its potential importance in practical applications. Besides, the Reynolds numbers encountered in most polymer processing applications are assumed to be negligible or at most small. Therefore, the boundary layer grows much faster than in Newtonian flows, and we can not make use of the abundant data previously obtained for Newtonian flows. Hence, to check the validity of the present method, we compared our numerical results for $R=1$ and $\epsilon=0.2$ with the analytical results obtained under the assumption that the fully developed flow ccondition has been obtained well within the streamwise coordinate $x=10$. The results showed an excellent agreement. We also considered the effect of the inlet velocity profile by using the plug flow at the inlet. The results did not seem to be affected very much, except that we had an unrealistically large value of the pressure at the entrance corner.

Since the consitutive equation for Oldroyd B fluid involves retardation time λ_2 as well as relaxation time λ_1, their ratio

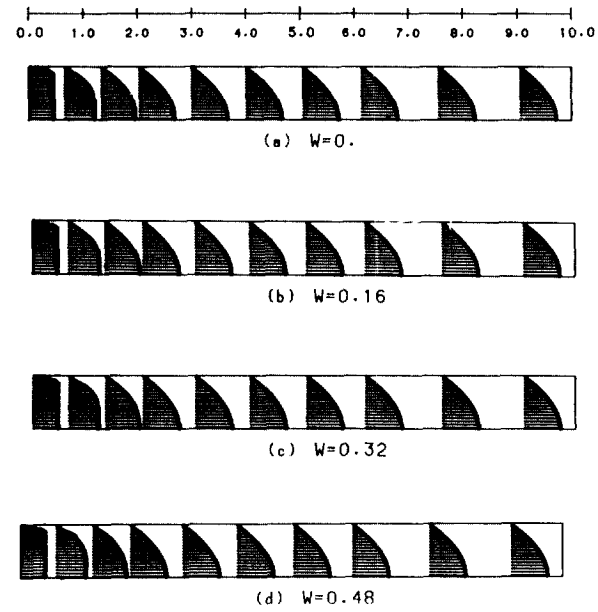

Fig. 4 Velocity profiles for $R=10$:(a) $W=0$; (b) $W=0.16$;(c) $W=0.32$; (d) $W=0.48$

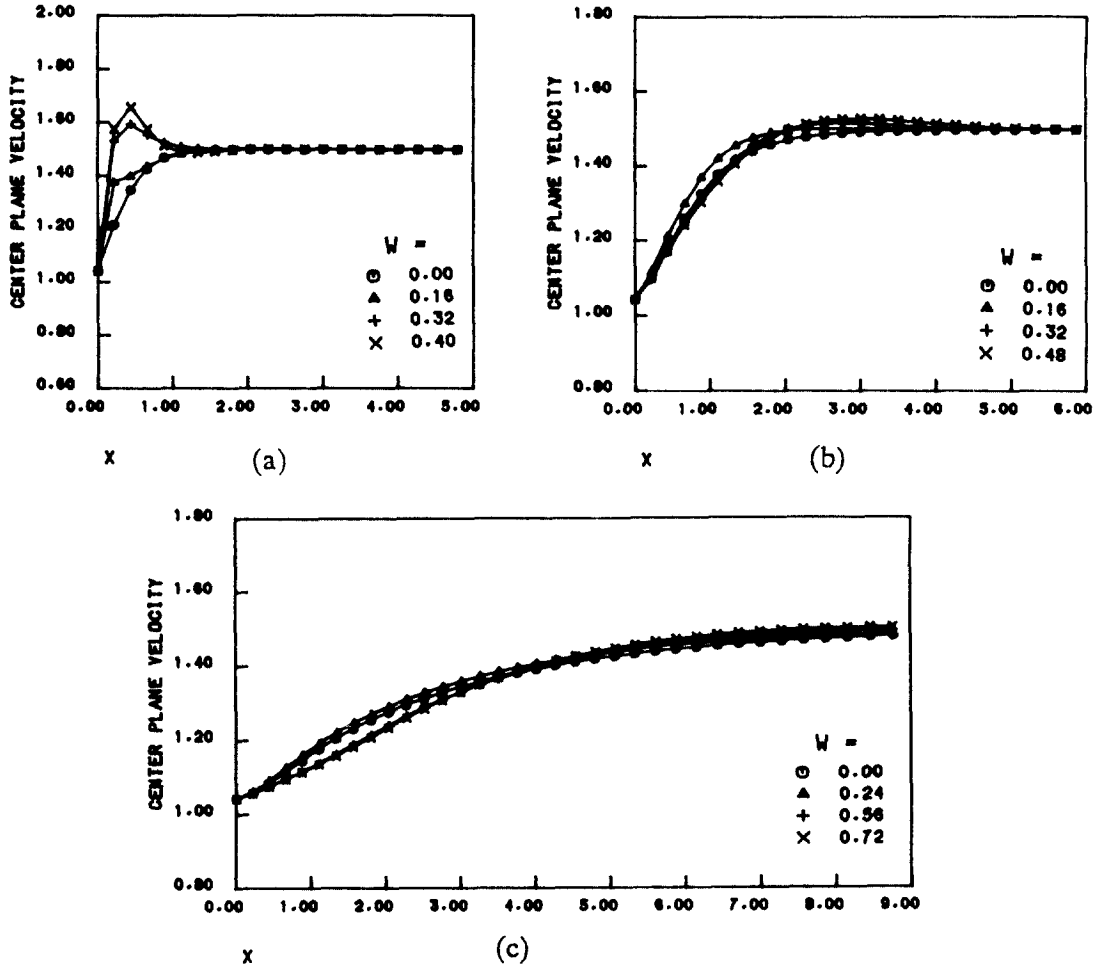

Fig. 5 Effect of the Weissenberg number on the center-plane velocity:(a) $R=0$; (b) $R=10$;(c) $R=50$

$\epsilon=\lambda_2/\lambda_1$ has to be assigned in performing numerical simulations. It is known that the only restriction on ϵ for Oldroyd B model is $0<\epsilon<1$, while that for Oldroyd 8-constant model is $1/9<\epsilon<1$(Lagnado et al., 1985). Therefore, in the present study, we arbitrarily choose $\epsilon=0.2$ and mainly consider the effect of the Weissenberg number W and the Reynolds number R. The effect of varying values of retardation time, i.e., ϵ will be considered in a continued study following the present one.

When ϵ is small, it can be seen that the Weissenberg number is mainly the ratio of stress relaxation time to flow characteristic time. Thus, increase of the Weissenberg number means increase of stress relaxation time at a fixed flow characteristic time. i.e., increase of long memory effect. As the Weissenberg number increases, significant changes in the developing velocity profile and in the distributions of pressure and stress components occur. Fig. 4 shows the developing velocity profiles for various values of W and for a fixed value of $R=10$. As the Weissenberg number increases, the entrance length slightly increases due to memory effect. However, as we examine the inertia effect by comparing the results obtained for $R=0$ and 50, the entrance length seems to be affected more by R than by W (Na, 1989).

This can be more clearly understood by examining the center plane velocity distributions, as shown in Fig. 5. Particular attention is called for the creeping flow case, Fig 5(a), where for larger values of W velocity overshoots can be observed. These are thought to occur due to strong memory effect which dominates completely over the inertia effect. However, as R increases (Figs. 5(b) and 5(c)), the inertia effect outweighs the elasticity effect and Newtonian fluid behavior becomes prevalent. This is in contrast to Gaidos and Darby (1988), who report that in all cases considered up to $R=100$, the solution converged to the fully developed profiles within $x=4$. Therefore, this needs further examination including the constitutive models used .

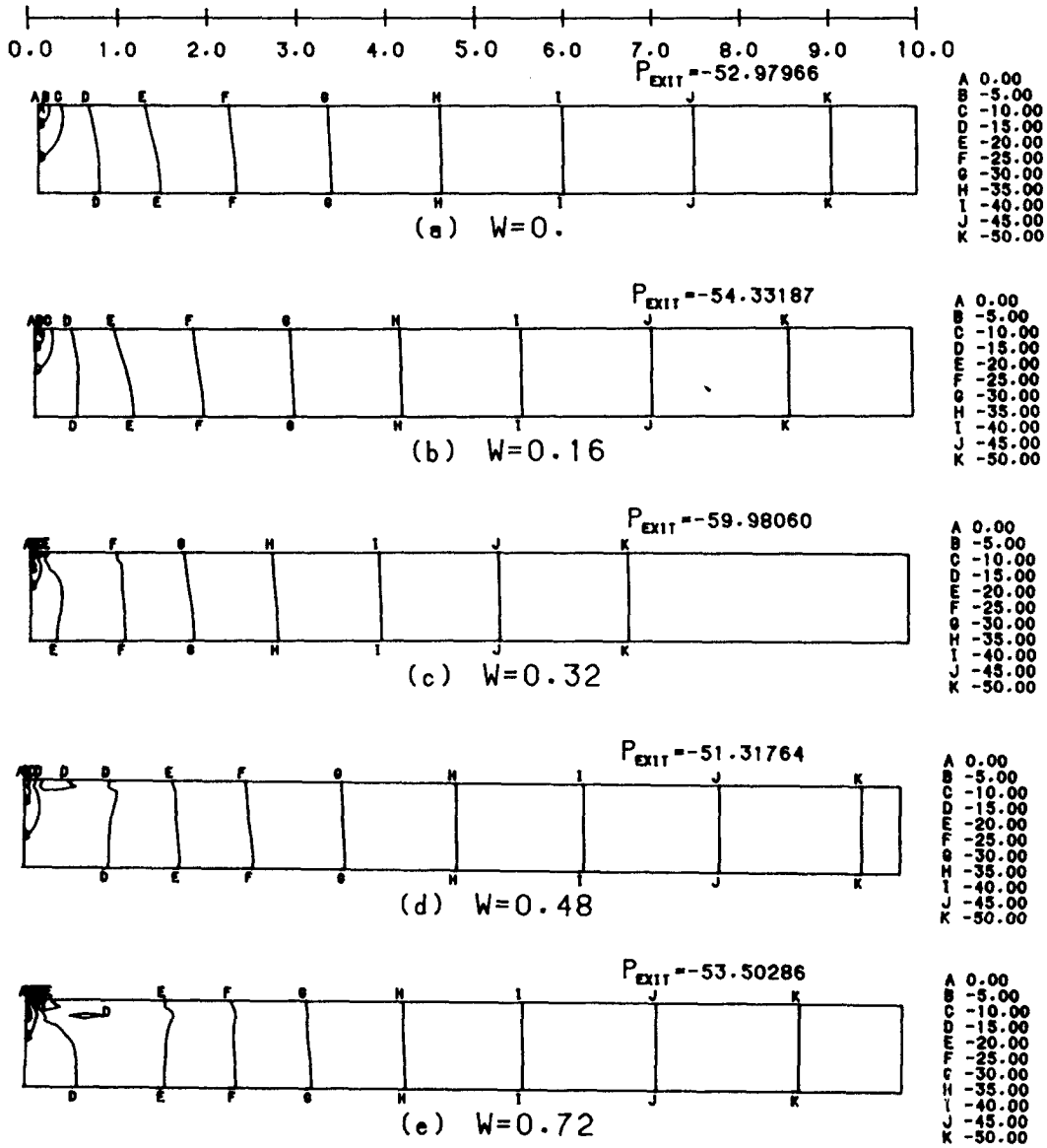

Fig. 6 Isobars obtained for $R=50$ of Oldroyd B model:(a) $W=0$; (b) $W=0.16$;(c) $W=0.32$; (d) $W=0.48$;(e) $W=0.72$

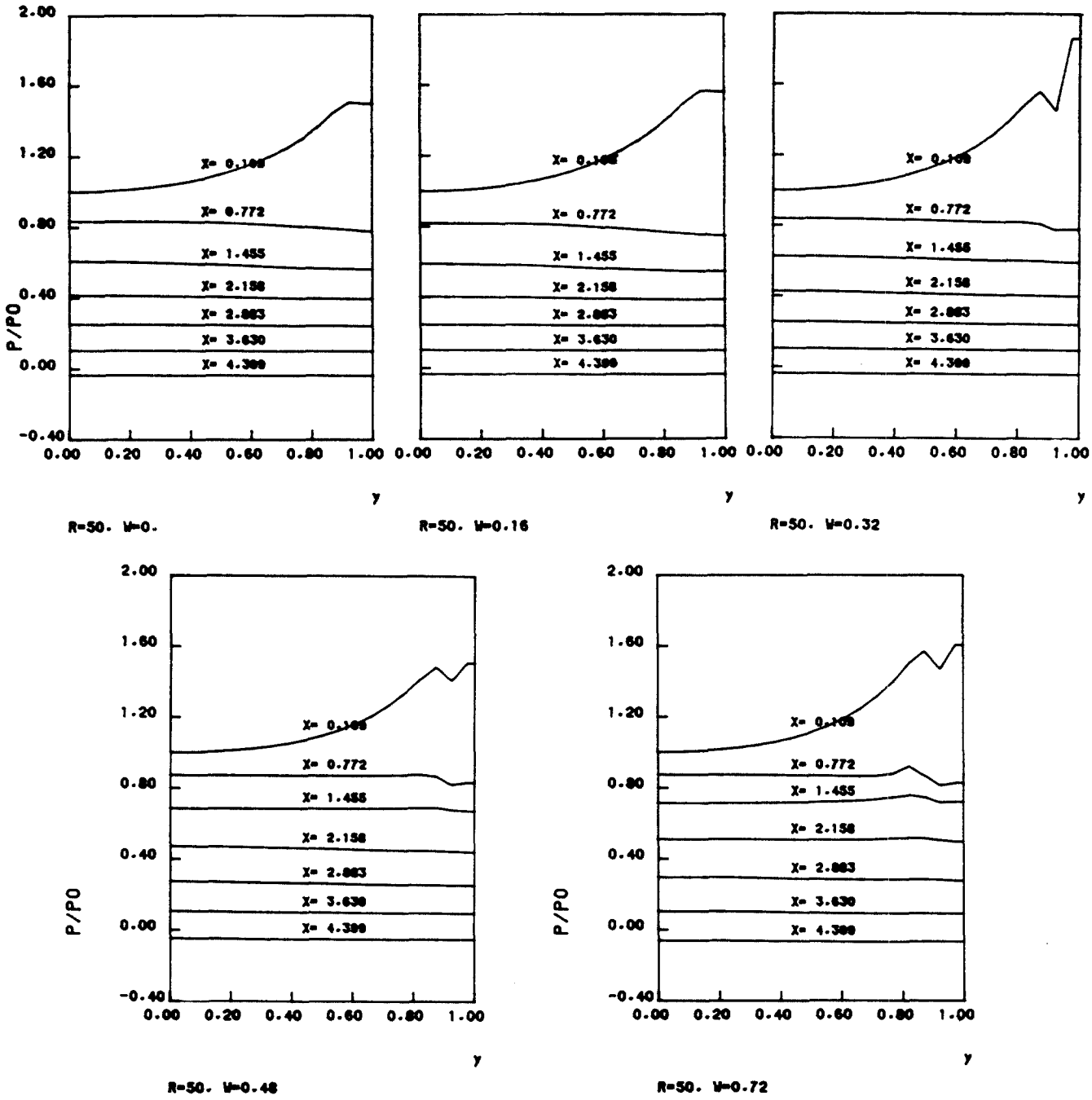

Fig. 7 Developing pressure distribution for $R=50$ of Oldroyd B model:(a) $W=0$; (b) $W=0.16$;(c) $W=0.32$; (d) $W=0.48$;(e) $W=0.72$

Figure 6 shows the isobars for $R=50$ and various values of W. In Fig. 7, a different representation of Fig. 6 is given, which shows the developing pressure distribution along downstream direction. Such figures may be used to estimate the values of the entrance length and the excess entrance pressure drop, if appropriate definitions are given. We also note that as the Reynolds number increases, the limiting Weissenberg number at which the breakdown of numerical convergence occurs also increases, which is in good qualitative agreement with Gaidos and Darby (1988). Further, it can be said that the pressure field near the inlet becomes unstable as the limiting Weissenberg number is reached.

In Figs. 8 and 9, the contour lines of the shear stress, τ and the first normal stress difference, σ-γ, are shown for $R=10$. When these figures are compared with those of Choi et al. (1988) which were obtained for the 4:1 contraction flow of a shear thinning fluid, we find general resemblance in the contour lines of τ, but much difference in the contour lines of σ-γ. Thus, it can be said that the distribution of the first normal stress difference in the entrance region is also important in determining whether a fluid is shear thinning or not. In any event, the characteristics of extensional flow are shown

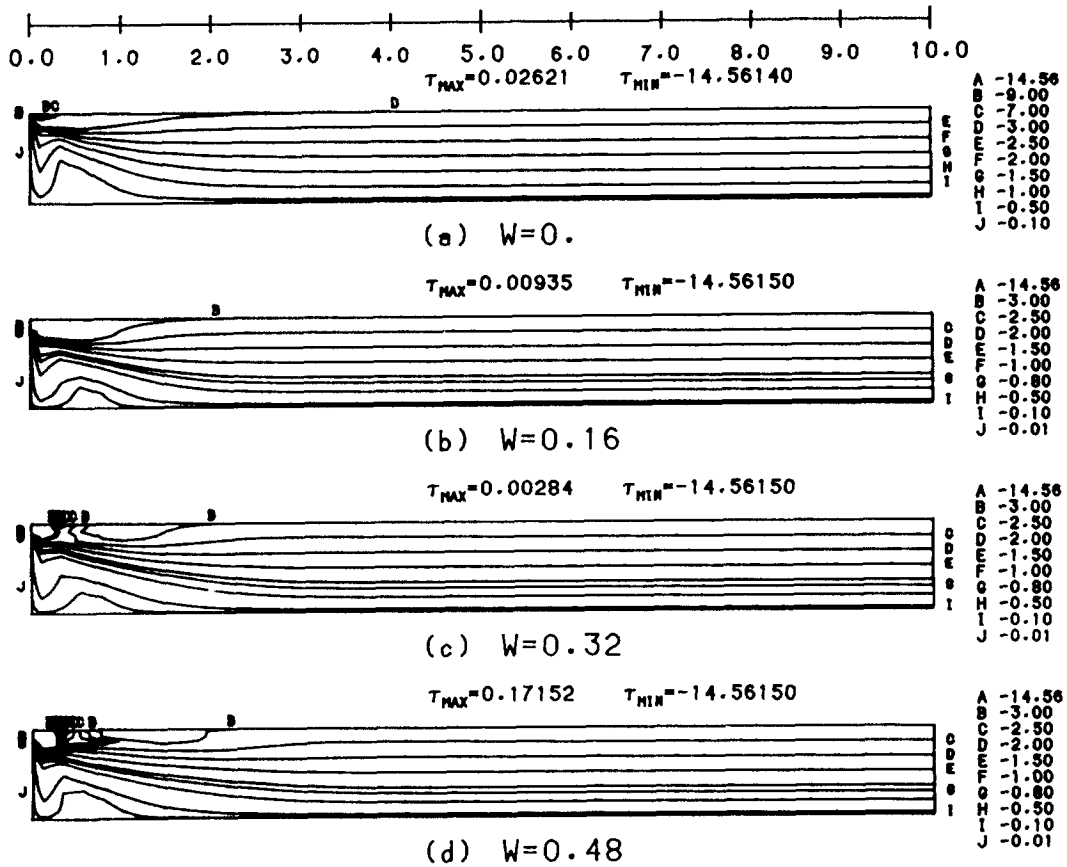

Fig. 8 Contour lines of the shear stress of $R=10$;(a) $W=0$;(b) $W=0.16$;(c) $W=0.32$;(d) $W=0.48$

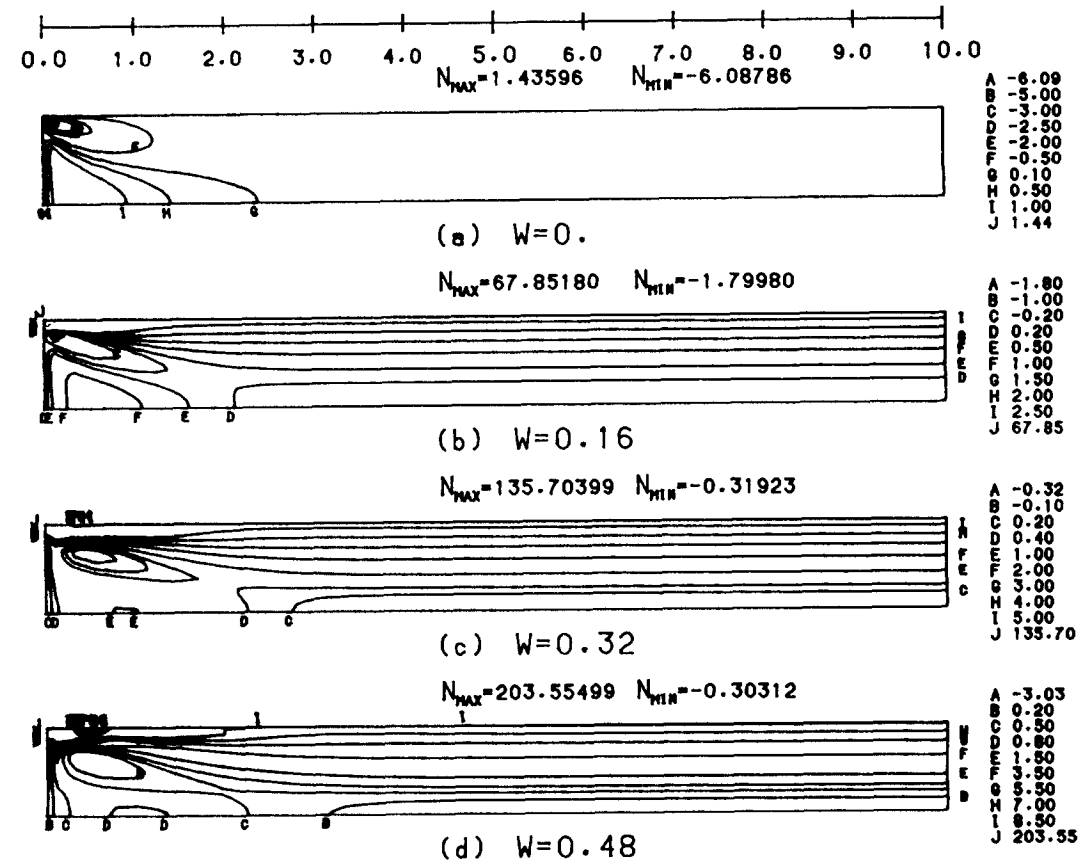

Fig. 9 Contour lines of the first normal stress difference for $R=10$:(a) $W=0$; (b) $W=0.16$;(c) $W=0.32$; (d) $W=0.48$

to be more predominant than those of shear flow in the entrance region, penetrating farther downstream as W increases.

5. CONCLUSION

A numerical simulation of the hydrodynamically developing flow of the Oldroyd B fluid has been performed by adopting SIMPLER algorithm in discretizing the momentum equations and an upwind corrected scheme in discretizing the constitutive equations on a non-uniform grid system. It has been shown that SIMPLER algorithm can be successfully applied for the numerical simulation of the flow of a viscoelastic fluid with retardation time by decomposing the stress into non-Newtonian and Newtonian parts. The entrance length increases slightly as the Weissenberg number increases for a fixed Reynolds number. However it is more affected by the Reynolds number than by the Weissenberg number. Velocity overshoots along the center plane appear for large values of the Weissenberg number in case of the creeping flow. The distributions of the shear stress and the first normal stress difference show clearly the development of the flow characteristics from extensional flow to shear flow.

REFERENCES

Chang, P.-W., Patten, T.W. and Finlayson, B.A., 1979, "Collocaton and Galerkin Finite Element Methods for Viscoelastic Fluid Flow- I ", Comput. Fluids, Vol. 7, pp. 267~283.

Choi, H.C., Song, J.H. and Yoo, J. Y., 1988, "Numerical Simulation of the Planar Contraction Flow of a Giesekus Fluid," J. Non-Newtonian Fluid Mech, Vol. 29, pp. 347~379.

Gaidos, R. E. and Darby, R., 1988, "Numerical Simulation and Change in type in the Developing Flow of a Nonlinear Viscoelastic Fluid", J. Non-Newtonian Fluid Mech. Vol. 29, pp. 59~79.

Joseph, D.D., Renardy, M. and Saut, J, -C., 1985, "Hyperbolicity and Change of type in the Flow of Viscoelastic Fluids," Arch. Rat. Mech Anal., Vol. 87, pp. 213~251.

Lagnado, R. R., Phan-Thien, N. and Leal, L. G., 1985, "The Stability of Two-Dimensional Linear Flows of an Oldroyd-Type Fluid," J. Non-Newtonian Fluid Mech., Vol. 18, pp. 25~59.

Mendelson, M.A., Yeh, P.-W., Brown, R.A. and Armstrong, R.C., 1982, "Approximation Error in Finite Element Calculation of Viscoelastic Fluid Flows", J.Non-Newtonian Fluid Mech., Vol. 10, pp. 31~54.

Na, Y., 1989, "Numerical Study on Channel Flows of Viscoelastic Fluid," M.S. thesis, Department of Mechanical Engineering, Seoul National University.

Patankar, S.V., 1980, "Numerical Heat Transfer and Fluid Flow", McGraw-Hill, New York, pp. 120~134.

Song, J.H. and Yoo, J.Y., 1987, "Numerical Simulation of Viscoelastic Flow through a Sudden Contraction Using a Type Dependent Difference Method", J. Non-Newtonian Fluid Mech., Vol. 24, No. 2, pp. 221~243.

Yoo, J.Y., Ahrens, M and Joseph, D.D., 1985, "Hyperbolicity and Change of Type in Sink Flow", J. Fluid Mech., Vol. 153, pp. 203~214.